

Maximum Wind Speed Changes over China

JIANG Ying^{1,2*} (江 滢), LUO Yong^{3,4} (罗 勇), and ZHAO Zongci^{3,4} (赵宗慈)

¹ Institute of Plateau Meteorology of CMA, Chengdu 610072

² Public Meteorological Service Center of CMA, Beijing 100081

³ Center for Earth System Science, Tsinghua University, Beijing 100084

⁴ National Climate Center of China, Beijing 100081

(Received October 19, 2011; in final form June 25, 2012)

ABSTRACT

In this study, the maximum wind speed (WS_{\max}) changes across China from 1956 to 2004 were analyzed based on observed station data, and the changes of WS_{\max} for 2046–2065 and 2080–2099 are projected using three global climate models (GFDL_CM2_0, CCCMA_CGCM3, and MRI_CGCM2) that have participated in the IPCC Fourth Assessment Report (AR4). The observed annual and seasonal WS_{\max} and the frequency of gale days showed obvious declining trends. The annual WS_{\max} decreased by approximately 1.46 m s^{-1} per decade, and the number of gale days decreased by 3.0 days per decade from 1956 to 2004. The amplitudes of the annual and seasonal WS_{\max} decreases are larger than those of the annual and seasonal average wind speeds (WS_{avg}). The weakening of the East Asian winter and summer monsoons is the cause for the distinct decreases of both WS_{\max} and WS_{avg} over the whole China. The decrease of WS_{\max} in the southeast coastal areas of China is related to the reduced intensity of cold waves in China and the decreasing number (and decreasing intensity) of land-falling typhoons originated in the Northwest Pacific Ocean.

The global climate models GFDL_CM2_0, MRI_CGCM2, and EBGCM (the ensemble of above mentioned three global climate models) consistently suggest that the annual and seasonal WS_{\max} values will decrease during 2046–2065 and 2080–2099 relative to 1981–2000. The models also suggest that decreases in WS_{\max} for whole China during 2046–2065 and 2080–2099 are related to both the reduced intensity of cold waves and the reduced intensity of the winter monsoon, and the decrease in WS_{\max} in the southeast coastal areas of China is corresponding to the decreasing number of tropical cyclones over the Northwest Pacific Ocean in the summer during the same periods.

Key words: maximum wind speed, change, projection, China

Citation: Jiang Ying, Luo Yong, and Zhao Zongci, 2013: Maximum wind speed changes over China. *Acta Meteor. Sinica*, **27**(1), 63–74, doi: 10.1007/s13351-013-0107-x.

1. Introduction

Over the last century, the earth's climate has been warming (Wang and Ye, 1995; IPCC, 2007). Global climate changes from 1906 to 2005 have led to increases in the annual mean surface temperature of approximately 0.74°C ($0.56\text{--}0.92^\circ\text{C}$), with a slightly larger increase in China compared to that of the global average. Climate model studies indicate that climate warming trends will continue over the next 50–100 years (IPCC, 2007; PRCC, 2007). Extreme climate change due to global warming is a unique and valuable research area (Yan and Yang, 2000). Research

regarding changes in maximum wind speeds (WS_{\max}) at the national level is important to sustainable utilization of wind energy and mitigation of disasters caused by extreme winds. It is also useful for planning wind energy industry development, maintaining electricity grid, and predicting the price of wind electricity.

Relevant studies have focused on two areas regarding the near-surface (10-m level) annual, seasonal, monthly, and daily changes of WS_{avg} (average wind) and WS_{\max} . The first area involves observational data analysis of the cause of wind changes, and the second area involves mathematical simulation and projection. Regarding observational data analysis, previous work

Supported by the Open Laboratory Fund of the Institute of Plateau Meteorology of China Meteorological Administration (CMA) (LPM2012005), National Natural Science Foundation of China (41205114), and CMA Special Public Welfare Research Fund (GYHY201106018 and GYHY200806009).

*Corresponding author: jiangy@cma.gov.cn.

©The Chinese Meteorological Society and Springer-Verlag Berlin Heidelberg 2013

suggested that there had been a decreasing trend of annual WS_{avg} over the past 50 years (Wang et al., 2004; Ren et al., 2005; Zhu and Liang, 2005; Xu et al., 2006; Zhou and Yu, 2006). Li et al. (2007) further indicated that the mean wind energy density in China between 1960 and 2000 exhibited declining trends, on both annual and seasonal scales. Yan and Yang (2000) showed that the maximum wind speed decreased by $1\text{--}3\text{ m s}^{-1}$ during the last few decades. Jiang et al. (2010a) indicated that WS_{avg} showed declining trends over broad areas of China, except the regions from the Hetao area to Yunnan Province and Guangxi Region. The annual WS_{avg} over China showed a decreasing trend with values of -0.12 , -0.10 , and -0.02 m s^{-1} per decade in the sounding data, the NCEP/NCAR and the ERA40 reanalysis data at 925 hPa, respectively, over the last 50 years. The primary reason for this decreasing trend is changes in the atmospheric circulation. Li et al. (2011) suggested that the major cause of the reduced wind speed observed during the past half century is the decreasing sea level pressure (SLP) gradients in North China. Most of the above-mentioned studies have focused on WS_{avg} in China, while some of the studies address WS_{max} but do not provide a clear explanation for the related changes. None of the previous studies include a future projection of WS_{max} (such as for the 21st century). Therefore, this study aims to examine the WS_{max} changes and the underlying reasons in both present and future China.

Since the 1990s, research on climate models has developed rapidly. Climate models have been employed to simulate and project variations in temperature and precipitation (Qian and Lin, 2004; Cook and Vizy, 2006; Phillips and Gleckler, 2006; IPCC, 2007; Zhang et al., 2008; Zhou et al., 2008; Yang et al., 2010; Hao et al., 2011). Scientists also used climate models to reproduce and project changes of near-surface wind and the corresponding energy. For example, Pryor et al. (2005), Rockel and Woth (2007), and Bloom et al. (2008) independently examined variations in near-surface wind and wind power density during the 21st century over northern Europe, Europe, southwestern coast of North America, and Mediterranean region. Jiang et al. (2009a, b, 2010b, c, d) projected changes

in WS_{avg} and wind power density over China. However, there have been few reports on the projected changes of WS_{max} in China. In this paper, based on features of future WS_{avg} changes, we analyze and project future changes in near-surface WS_{max} throughout China.

2. Data and methods

2.1 Data processing

2.1.1 Observation data

To investigate the effect of urbanization on long-term wind variations, two observational datasets were used. One dataset is from 745 basic and standard weather stations, and the other is from 2425 generic weather stations. Both datasets conform to the guidelines of the WMO global observation systems (WMO, 2004) and the China Meteorological Administration (CMA) technical observation standards (CMA, 2003). Wind data from 535 stations, with no missing records from 1956 to 2004, were used. These stations are evenly distributed, with the exception of a sparse distribution over the Tibetan Plateau. These datasets together with dust storm data and sounding data from 140 stations were obtained from instruments operated by the NMIC (National Meteorological Information Center of CMA). The number of typhoons originated in western Pacific that either made landfall or influenced wind speeds was also obtained from the NMIC. Cold wave days were defined based on the National Climate Center of CMA standards (Wang and Ding, 2006).

For analysis of wind speed characteristics in the mid and low troposphere, wind speed at the surface level, 925, 850, and 700 hPa from the NCEP and ERA40 reanalysis datasets were also used (see Table 1).

The near-surface layer is defined as 10 m above ground, and WS_{avg} represents the average wind speed from four-time daily observed values and was averaged over a particular time period (day, month, or year). The maximum value from all 10-min average wind speeds in a particular time period (day, month, or year) is defined as observed (daily, monthly, or yearly)

Table 1. Data time periods under SRES A2 for various simulation and observation datasets

Data	20th century	21st century (middle stage)	21st century (late stage)
GFDL_CM2_0, CCCMA_CGCM3, and MRI_CGCM2	1956–2000	2046–2065	2080–2099
NCEP/NCAR	1965–2004	/	/
ERA40	1958–2001	/	/
Sounding	1980–2004	/	/
Surface observation	1965–2004	/	/

WS_{\max} . Gale days are defined as days with wind speed $\geq 17 \text{ m s}^{-1}$, as determined with direct measurements, or those at the eighth grade or higher, as determined with visual observations when there is instrument failure.

2.1.2 Model data

Since the three global climate models, i.e., GFDL_CM2_0 from the NOAA Geophysical Fluid Dynamics Laboratory, CCCMA_CGCM3 from the Canadian Centre for Climate Modeling and Analysis, and MRI_CGCM2 from the Japan Meteorological Research Institute, have strong ability to simulate current wind speeds in China (Jiang et al., 2009b), these three models with an emission projection of SRES A2 were employed to project annual and seasonal WS_{\max} values over China for periods 2046–2065 and 2080–2099.

Considering the limitations of the simulated output datasets from the GCMs, the yearly (or monthly) WS_{\max} is defined as the maximum value among the daily average wind speeds. EBGCM denotes the ensemble of the above three global climate models.

2.2 Computation method

Global climate models (GCMs) differ in their resolution. For comparative purposes, outputs of GCMs and observations of related stations were interpolated onto $1.0^\circ \times 1.0^\circ$ grids using the inverse distance weight method.

To determine the 21st century WS_{\max} , projections of each model were compared to corresponding 20th century data, and the difference of wind speed was calculated between the 20th and 21st century. To examine the long-term changes of WS_{\max} and gale days, we use linear regression trend analysis (Wei, 1999) followed by a significance test of the WS_{\max} trend in terms of space-time variability correlation co-

efficients.

To address the detailed characteristics of WS_{\max} changes in various regions and to compare these values with those of WS_{avg} (Jiang et al., 2010a), we divide the experimental area into 12 sub-regions based on topography and physiognomy. The stations in every sub-region are evenly distributed. The 12 sub-regions are: (1) Xinjiang, (2) west Inner Mongolia, (3) east Inner Mongolia, (4) Northeast China, (5) Tibetan Plateau, (6) west-central China, (7) east-central China, (8) the northeastern coast of China, (9) Yunnan, (10) Guizhou, (11) South China, and (12) southeastern coast of China.

The WS_{\max} in January, April, July, and October was used to represent seasonal values of winter, spring, summer, and autumn, respectively.

3. Observed maximum wind changes in China during 1956–2004 and associated causes

3.1 Variations of maximum wind

We found that the 50-yr annual WS_{\max} exhibited a noticeable decline (the solid line in Fig. 1a) of approximately -1.46 m s^{-1} per decade, with a 23.6% decrease per decade and a significant linear trend (at the 0.001 level). The annual WS_{avg} over China declined after 1956 by approximately -0.124 m s^{-1} per decade, with a 5.17% decrease per decade (Jiang et al., 2010a). The amplitude of the WS_{\max} decrease is larger than that of the WS_{avg} decrease. This trend is consistent with that found by Yan and Yang (2000). The mean frequency of annual gale days displayed a remarkable decrease over the last 50 years, with -3.0 gale days per decade, corresponding to a -12.7% decrease per decade.

Seasonally, WS_{\max} declined within the study period, and it decreased more significantly during spring

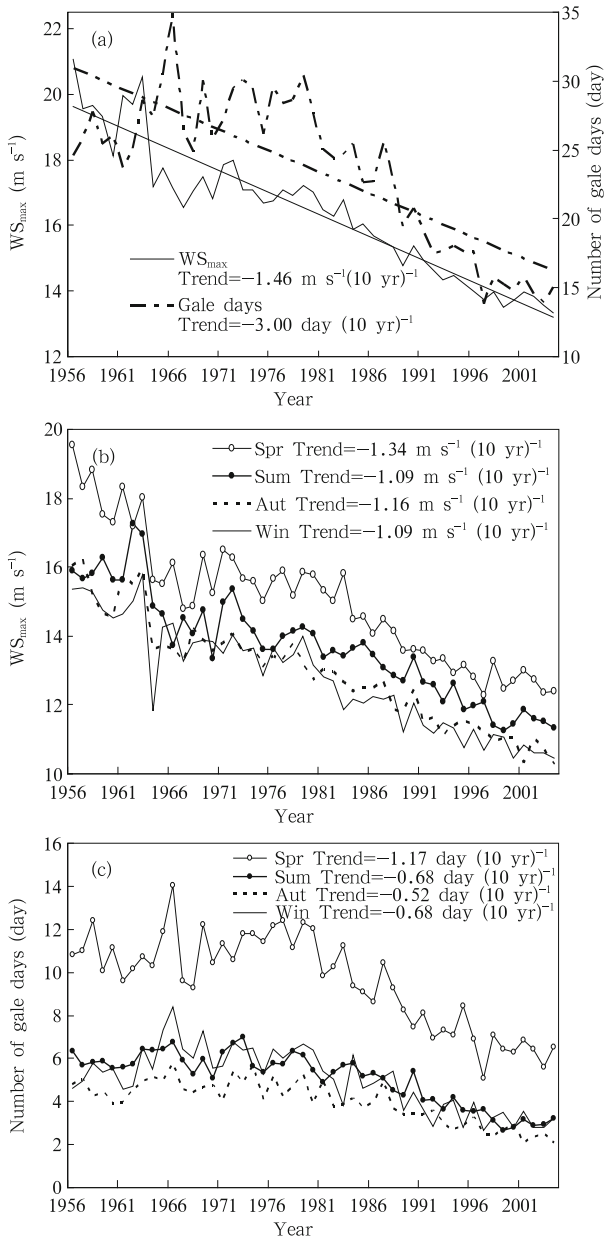


Fig. 1. Observed annual (seasonal) maximum wind ($m s^{-1}$) and gale days (day) in China during 1956–2004. (a) Annual maximum wind (solid line) and gale days (dotted line), (b) seasonal maximum wind, and (c) seasonal gale days.

(Fig. 1b). The frequency of gale days decreased as well (Fig. 1c), with spring exhibiting the strongest winds, the highest gale frequency, and a marked decrease in the value of strongest wind speed and the number of windy days. In this case, WS_{max} does not follow the trends of WS_{avg} .

Both annual WS_{max} and WS_{avg} decreased over most of China during 1956–2004 (see Fig. 2). The declining trend of WS_{max} is more significant than that of WS_{avg} . However, there is a difference in the trend distribution between WS_{max} and WS_{avg} . The yearly WS_{avg} exhibited a large decline across China, except in the Hetao area southward to Yunnan and Guangxi and in eastern Tibet, where there were no significant trends in wind change (Jiang et al., 2010a). Examination of the distribution of WS_{avg} showed that the zones with a decline of WS_{avg} ($< -0.12 m s^{-1}$ per decade) also exhibited greater long-term average wind speeds ($> 2.2 m s^{-1}$), and the zones with no noticeable trends corresponded to those of multiple-year average weak winds, implying that the yearly WS_{avg} decreases occurred primarily in regions with greater wind velocities (Jiang et al., 2010a). However, WS_{max} has different trend distribution characteristics. WS_{max} exhibited an obvious reduced trend across China. WS_{max} showed relatively small decreases (approximately $-0.8 m s^{-1}$ per decade) from western Inner Mongolia to Sichuan Province. WS_{max} exhibited relatively large decreases ($> -1.6 m s^{-1}$ per decade) in the regions from eastern Inner Mongolia to Fujian and Hainan provinces and across most regions of Northeast China. The regions with the smallest and largest WS_{max} decreases mismatched the regions with the smallest and largest decreases in WS_{avg} .

To further investigate regional wind characteristics during 1956–2004, the experimental area (i.e., China) was separated into 12 sub-regions (Jiang et al., 2010a). Both annual WS_{max} and the frequency of annual gale days exhibit declining trends (Table 2). WS_{max} decreased over northern (sub-regions 1–4) and southeast coastal China (sub-region 12), where the multi-year average wind speed is significantly greater than that in sub-regions 6 or 10. This is similar to the results of the annual WS_{avg} , but sub-regions 6 and 10 show decreases in WS_{max} and no significant trend or a slight increasing trend for WS_{avg} . However, the frequency of gale days differs between cases (Table 2), e.g., changes in WS_{avg} are closely related to changes in WS_{max} but not clearly related to the frequency of gale days. The latter denotes the frequency of extreme wind rather than the wind speed value.

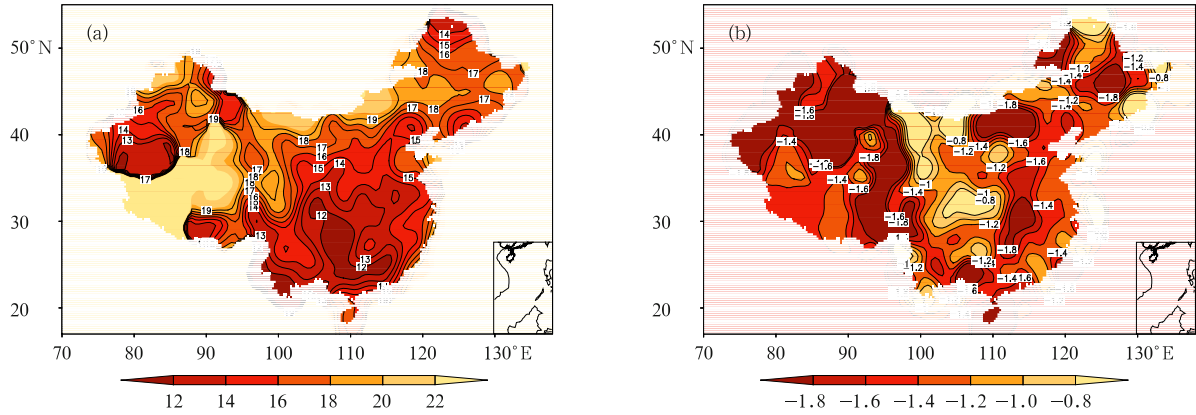


Fig. 2. Distributions of observed maximum and average wind speeds and trends during 1956–2004. (a) Maximum wind (m s^{-1}) and (b) trend of the maximum wind speed ($\text{m s}^{-1} (10 \text{ yr})^{-1}$).

Table 2. Annual maximum wind speed, average wind speed, number of gale days and their trends for the 12 sub-regions based on observation data in 1956–2004

Sub-regions	Maximum wind speed		Average (day)	Number of gale days		Average wind speed	
	Average (m s^{-1})	Trend ($\text{m s}^{-1} (10 \text{ yr})^{-1}$)		Trend ($\text{day} (10 \text{ yr})^{-1}$)	Trend ($\text{m s}^{-1} (10 \text{ yr})^{-1}$)		
1	17.3	-1.33 (7.69%)	29.8	-3.43 (11.51%)	-0.15 (6.25%)		
2	16.6	-1.22 (7.35%)	27.1	-5.38 (19.85%)	-0.20 (7.41%)		
3	18.1	-1.49 (8.23%)	42.6	-7.11 (16.69%)	-0.17 (5.86%)		
4	18.3	-1.73 (9.45%)	23.4	-3.58 (15.30%)	-0.15 (4.95%)		
5	17.7	-1.52 (8.59%)	59.2	-2.34 (3.95%)	-0.03 (1.32%)		
6	14.4	-0.69 (4.79%)	13.2	-1.30 (9.85%)	-0.02 (1.12%)		
7	14.9	-1.32 (8.86%)	14.4	-2.83 (19.65%)	-0.17 (6.91%)		
8	16.8	-0.85 (5.06%)	25.1	-4.40 (19.53%)	-0.16 (4.94%)		
9	12.9	-1.41 (10.93%)	15.3	-2.20 (14.38%)	-0.09 (5.03%)		
10	12.6	-0.86 (6.83%)	7.1	-2.22 (31.27%)	0.0 (0.0%)		
11	13.1	-1.04 (7.94%)	9.8	-1.96 (20.00%)	-0.10 (5.32%)		
12	17.2	-1.28 (7.44%)	18.1	-3.82 (21.10%)	-0.18 (6.14%)		
China	16.4	-1.46 (23.56%)	23.6	-3.00 (12.73%)	-0.124 (5.17%)		

WS_{\max} over sub-regions 1–4 is mainly impacted by cold waves during winter and spring. The declining trend over sub-regions 1–2 is more obvious than that over sub-regions 3–4. This finding represents the slightly different changes of cold wave intensity between the western (1–2) and eastern (3–4) sub-regions. For the regions along the southeast coast (8 and 12), WS_{\max} is primarily impacted by typhoons from the Northwest Pacific Ocean that either make landfall or influence wind speeds over land. The decrease in WS_{\max} over the southern sub-region (12) is more significant than that over the northern sub-region (8), which is related to the decrease of typhoon intensity

and frequency as well as the trajectories of typhoons traveling northward (Lei et al., 2009; Wang et al., 2006).

3.2 Causes of maximum wind decreases in China

3.2.1 Impact of wind instrument renewal and station shifting

Wind instrument renewal occurred in China during approximately 1969–1970, consistent with a time of significant changes in average wind measurements compared with wind measurements before and after the renewal events (Jiang et al., 2010a). However, the

change in maximum wind speed during the shift period is not clear. Ignoring the impact of national wind instrument renewal from 1969 to 1970, the maximum wind speed and gale day frequency significantly and gradually decreased from 1971 to 2004 (Fig. 1a). Additionally, the small number of stations undergoing instrument renewal and shifting did not affect the trends for the other 535 stations in the country. Thus, the effects of instrument renewing and station shifting are unlikely to significantly influence WS_{\max} changing trends.

3.2.2 Impact of urbanization

To explore the long-term effect of urbanization near climate stations on wind changes by using the method presented by Jiang et al. (2010a), we selected 174 of the 535 stations located near highly urbanized areas (urban stations) and 180 stations surrounded by areas with little or no urbanization (rural stations). These two sets of stations are evenly distributed, respectively, with the exception of a sparse distribution over the Tibetan Plateau. A comparison of the long-term changes in annual WS_{\max} (Fig. 3a) between the urban and rural stations reveals that WS_{\max} of urban stations was commensurate with that of rural stations before the 1970s, where both showed slightly declining trends over time. However, after the 1970s, WS_{\max} showed a prominent decreasing trend at both urban and rural stations. Additionally, the reducing trend was larger at urban stations than at rural stations (-1.75 versus -1.30 $m\ s^{-1}$ per decade). This is because the WS_{\max} trends did not differ initially between urban and rural stations due to the low construction frequency around both types of stations before the 1970s, but after the 1970s, the urban wind decline was

slightly greater than the rural wind decline due to enhanced urbanization that occurred rapidly post 1970 in China. However, even the stations that underwent little or no urbanization displayed a declining trend of annual WS_{\max} . This suggests that urbanization is unlikely to be a major factor affecting the yearly WS_{\max} decline in China, which is consistent with the findings of Jiang et al. (2010a) regarding WS_{avg} and those of Li et al. (2011) regarding extreme wind speeds in Beijing.

3.2.3 Upper-level wind changes

The average wind trends over China were calculated for winds measured at 10 m above ground and at different levels of the troposphere using NCEP/NCAR (1980–2004), ERA40 (1980–2001), and atmospheric sounding (1980–2004) data. Despite the differences in these data sources, consistent decreasing trends in wind speed are shown from 150 hPa to the surface. The decreasing wind speed detected from atmospheric soundings was the most significant at 250 hPa, with a decrease of -0.23 $m\ s^{-1}$ per decade. The declining wind trend gradually receded until the 850-hPa level, where there was a decrease of -0.04 $m\ s^{-1}$ per decade (Zhang et al., 2009). The three datasets obtained from NCEP/NCAR, ERA40, and atmospheric soundings yielded similar conclusions and exhibited similar trend values at the same level. Therefore, the decreasing winds in the near-surface layer are related to the decreasing winds in the troposphere and lower stratosphere over China (Fig. 4).

3.2.4 Impacts of atmospheric circulation and East Asian monsoon

Most of China is affected by the East Asian monsoons. The Asian zonal (meridional) circulation has

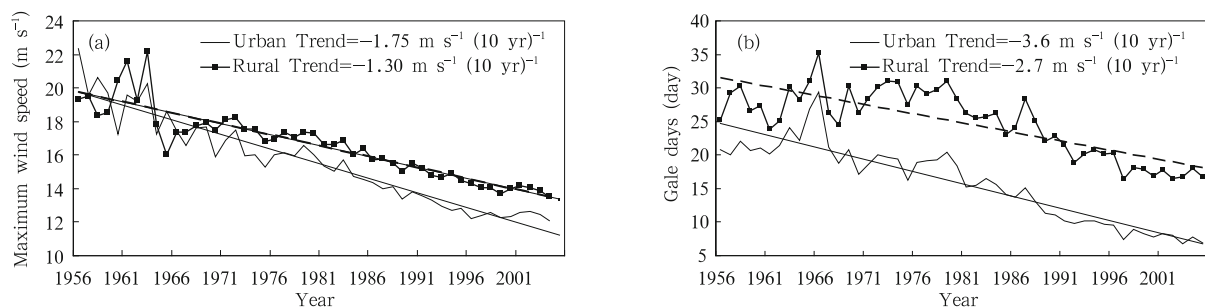


Fig. 3. Observed annual maximum wind speed (a; $m\ s^{-1}$) and frequency of gale days (b; day) over the urban stations (solid line) and rural stations (line with squares) during 1956–2004.

weakened over the past 50 years and resulted in weakened monsoons, which is consistent with the results that show reduced intensity of the winter and summer monsoons (Guo, 1983; Shi, 1996; Wang et al., 2001; Zhao and Zhou, 2005; IPCC, 2007). This suggests that, under the global warming, the air-sea thermal contrast decreases, the strength of the winter Siberian high is reduced (Guo et al., 2001; Guo et al., 2004) and thus, the atmospheric circulation varies accordingly. These factors are most likely the forces that cause the decline of yearly and seasonal maximal wind speed trends across China.

3.2.5 Association of cold waves, dust storms, and extratropical cyclones

Most of China is located in the midlatitudes of the Northern Hemisphere. In the last 50 years, the frequency of cyclones in the midlatitudes has decreased, and cyclone routes show a northward migration trend (Wang et al., 2007), which is closely related to declines in WS_{max} and gale day frequency in northern China. Extremely cold weather is often accompanied by a sharp temperature drop. During the study period, due to conspicuous warming in many regions of the extratropical latitudes, the number of cold wave days greatly decreased, which was linked to the reduced frequency of gale days (Wang and Ding, 2006; Qian and Zhang, 2007; Wei and Lin, 2009). Dust storms occur when large volumes of sand and dust are raised by strong winds and lead to sharply diminished visibility. The frequency of dust storm days is

associated with the frequency of gale days in much of northern China. The frequency of dust storm days has greatly reduced during the last 50 years (Qian et al., 2002; Ding et al., 2005; Wang et al., 2009). Due to global warming, the frequencies of cold waves, dust storms, and extratropical cyclone days have declined, which is the direct and convincing evidence of decreasing maximum winds.

3.2.6 Influences of northwestern Pacific typhoons along the southeast coast of China

Typhoons in the Northwest Pacific Ocean have an important climatological influence, especially those that make landfall on the southeast coastal regions of China. Typhoons often bring disastrous winds. Based on the observation data, the frequency of typhoons has significantly declined (Fig. 5). This finding is consistent with previous research (Ren et al., 2006; Wang

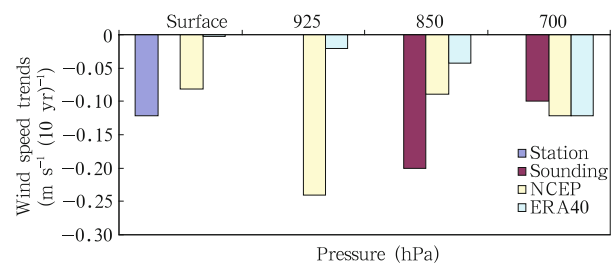


Fig. 4. Wind speed changes over China based on the observed station data (dark blue), sounding data (red), NCEP reanalysis data (yellow), and ERA-40 reanalysis data (light blue) in the mid-low troposphere from 1956 to 2004.

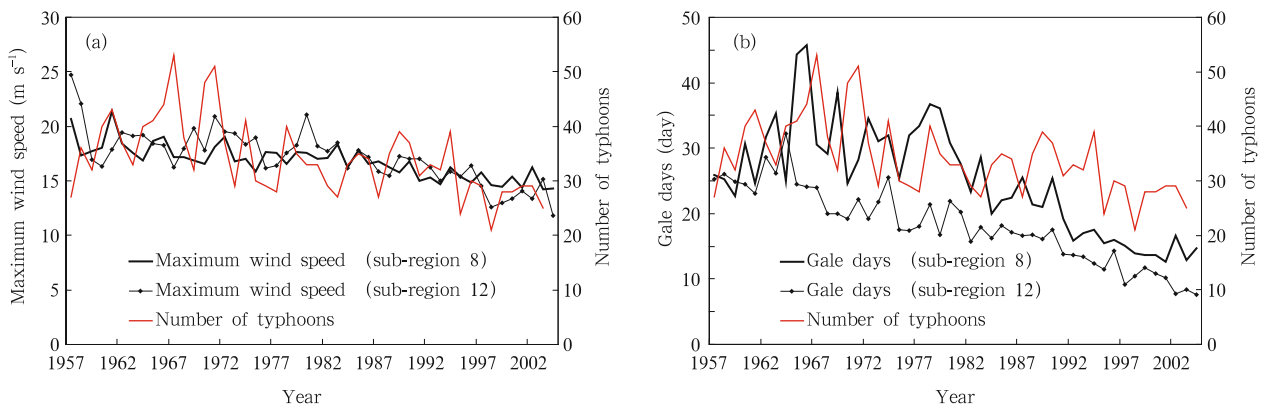


Fig. 5. Changes in the observed annual maximum wind speed (a; $m s^{-1}$) and frequency of gale days (b; day) for sub-regions 8 and 12 located along the east coast of China, and the number of typhoons in the western Pacific (red line) from 1956 to 2004.

et al., 2006; Wang and Zhang, 2006; Hu and Song, 2009). Previous studies also indicate that the strength of strong typhoons has weakened during the last 50 years (Emanuel, 2005; Wu et al., 2007; James et al., 2008). Figure 5 shows that the gale day frequency in sub-regions 8 and 12 correlates with the frequency of typhoon activity in the Northwest Pacific Ocean with coefficients of 0.46 and 0.56 at the 99.9% significance level, respectively. Thus, the declining trend of both the frequency and strength of typhoons in the Northwest Pacific Ocean is closely related to the decreases in WS_{\max} and the frequency of gale days in the south-east coastal areas of China.

3.2.7 Correlation between temperature increases in China and maximum wind changes

Global warming can cause significant extreme event feature changes (Ding et al., 2002; IPCC, 2007; PRCC, 2007). For example, during the last 50 years, studies have shown slight increases in maximum temperature, significant increases in minimum temperature, increases in frequency and strength of extreme precipitation, decreases in dust storm frequency (closely related to increased rainfall), and decreases in frequency of strong wind events in China (Wang and Zhai, 2004). Li et al. (2011) also showed that the changes in strong winds or wind speed extremes are due to large-scale climate changes in the region. Therefore, global warming, especially in the mid and high latitudes of the Northern Hemisphere, results in decreasing temperature differences between the Northern and Southern Hemispheres, declines in atmospheric baroclinicity, decreasing SLP gradient, possible decreases in the frequency of gale and cold wave days, and subsequently, reduced WS_{\max} in China. This is only the statistical relationship between global (or regional) warming and maximum wind speed changes over China. The mechanism of maximum wind speed changes caused by global (or regional) warming is not clear. Further research is needed to provide a more dynamic explanation.

4. Climate model-projected changes in maximum wind speed across China during the late 21st century

Several studies utilizing GCMs over the last sev-

eral decades have indicated that the GFDL_CM2_0, MRI_CGCM2, and CCCMA_CGCM3 models are able to simulate wind (at the 10-m level) and temperature changes in China (Wang et al., 2001; Zhou and Yu, 2006; IPCC, 2007; PRCC, 2007; Zhao et al., 2007; Jiang et al., 2009a, 2010b). These three global climate models are now used to project wind features, such as WS_{\max} , throughout China during the late 21st century.

4.1 2046–2065 projection

The annual WS_{\max} throughout China between 2046 and 2065, as projected by both GFDL_CM2_0 and MRI_CGCM2, is likely to decrease by -4.80 and -4.55 $m\ s^{-1}$, respectively, relative to the 1981–2000 value (7.0 and 6.5 $m\ s^{-1}$, respectively). However, the CCCMA_CGCM3 model projects a slight increase in WS_{\max} of $+0.35$ $m\ s^{-1}$. The combined results from these three models indicate that WS_{\max} will decrease by approximately -3.0 $m\ s^{-1}$ per year from 2046 to 2065 relative to the 1981–2000 value (8.5 $m\ s^{-1}$) (see Table 3).

In each season, both GFDL_CM2_0 and MRI_CGCM2 project WS_{\max} to be lower during 2046–2065 by a range from -1.90 to -3.71 $m\ s^{-1}$ relative to the 1981–2000 value, with the largest differences occurring in summer and autumn. The combined results from GFDL_CM2_0, MRI_CGCM2, and CCCMA_CGCM3 project WS_{\max} to be lower in 2046–2065 by a range from -1.35 to -2.46 $m\ s^{-1}$ relative to the 1981–2000 value. The range of WS_{\max} decreases is more significant than that of the WS_{avg} decreases (Table 3).

4.2 2080–2099 projection

The characteristics of the annual WS_{\max} change during 2080–2099 are similar to those during 2046–2065. The GFDL_CM2_0 and MRI_CGCM2 models, as well as the combined model results, show a clear declining trend compared to that from 1981 to 2000, while the CCCMA_CGCM3 model shows a slight increasing trend. The range of WS_{\max} decreases during the 2080–2099 period is more significant than that of WS_{avg} (Table 3).

Notably, the ranges of the four seasonal WS_{\max} decreases during the 2080–2099 period, as projected

Table 3. Wind speed changes (WS_{avg} and WS_{max} ; $m\ s^{-1}$) as projected by three GCMs and their ensemble under SRES A2 for 2046–2065 and 2080–2099 relative to 1981–2000

		GFDL_CM2_0		MRI_CGCM2		CCCMA_CGCM3		EBGCM	
		WS_{avg}	WS_{max}	WS_{avg}	WS_{max}	WS_{avg}	WS_{max}	WS_{avg}	WS_{max}
2046–2065	Jan.	0.00/1.7	-2.20/5.5	-0.12/1.9	-1.90/6.9	-0.15/3.2	0.05/7.9	-0.09/2.3	-1.35/6.8
	Apr.	0.05/1.3	-2.96/6.2	-0.11/2.0	-2.64/6.7	-0.52/2.8	0.18/9.6	-0.19/2.0	-1.81/7.5
	Jul.	0.02/1.0	-3.52/6.3	-0.11/1.4	-3.71/5.7	-0.13/0.8	0.09/11.0	-0.07/1.1	-2.38/7.7
	Oct.	0.01/1.3	-3.63/6.7	0.22/1.7	-3.62/6.2	0.16/1.6	-0.12/12.4	0.13/1.6	-2.46/8.4
	Year	-0.02/1.4	-4.80/7.0	-0.05/1.8	-4.55/6.5	-0.06/2.3	0.35/12.0	-0.04/1.8	-3.00/8.5
2080–2099	Jan.	-0.09/1.7	-2.29/5.5	-0.13/1.9	-1.83/6.9	-0.20/3.2	0.23/7.9	-0.14/2.3	-1.30/6.8
	Apr.	0.01/1.3	-3.06/6.2	-0.17/2.0	-2.79/6.7	-0.61/2.8	0.34/9.6	-0.26/2.0	-1.84/7.5
	Jul.	0.10/1.0	-3.55/6.3	-0.16/1.4	-3.80/5.7	-0.22/0.8	0.20/11.0	-0.09/1.1	-2.38/7.7
	Oct.	-0.05/1.3	-3.61/6.7	0.13/1.7	-3.60/6.2	0.11/1.6	0.08/12.4	0.06/1.6	-2.38/8.4
	Year	-0.05/1.4	-4.83/7.0	-0.07/1.8	-4.57/6.5	-0.11/2.3	0.35/12.0	-0.08/1.8	-3.02/8.5

Note: the average wind speed value for 1981–2000 is written after the ‘/’, and the difference between values from 2046–2065 (or 2080–2099) and 1981–2000 is written in front of the ‘/’. EBGCM is the ensemble of GFDL_CM2_0, MRI_CGCM2, and CCCMA_CGCM3.

by the three GCMs and the ensemble of the models, are similar to the projected ranges during the period 2046–2065 (Table 3).

Several studies showed that, with regard to global warming, the frequency of cold waves accompanying the East Asian winter monsoon will decrease during the 21st century (Hu et al., 2000; Bueh et al., 2003; IPCC, 2007). The decreased frequency of cold waves likely drives the declines in WS_{avg} and, in particular, WS_{max} . The changes in WS_{max} may also be related to specific extreme events, such as cold waves, dust storms, and typhoons. The frequency of cold waves will likely decrease during the 21st century (IPCC, 2007). Approximately 10 climate models that include anthropogenic emission data have predicted that, after CO_2 doubling, the frequency of tropical cyclones over the Northwest Pacific Ocean is likely to decrease by the end of the 21st century (Zhao et al., 2007) and the frequency of typhoons over the western Pacific Ocean making landfall in China might decrease as well (Knutson and Tuleya, 1999; Knutson et al., 2001; Gao et al., 2002, 2003; IPCC, 2007). Therefore, decreases in WS_{max} over China during the 21st century are related to future decreases of cold waves, and decreases in WS_{max} over the southeast coastal areas of China during the 21st century are corresponding to future decreases of typhoons.

5. Concluding remarks

Based on the observation data, it is found that

annual and seasonal WS_{max} , frequency of gale days, and wind speed in the troposphere and lower stratosphere declined from 1956 to 2004 (especially in winter) in China. The amplitudes of annual and seasonal WS_{max} decreases were more significant than those of WS_{avg} , especially in spring.

Wind instrument renewal, station shifting, and urbanization are not major factors affecting the yearly WS_{max} decline in China. The decreasing intensity of the East Asian winter and summer monsoons results in the decrease in the annual and seasonal WS_{max} and WS_{avg} . The distinct decrease of cold waves in China is a key factor for the distinct decrease in annual and seasonal WS_{max} in whole China, and the declining frequency of typhoons making landfall were key factors for the distinct decrease in annual and seasonal WS_{max} in the southeast coastal areas of China between 1956 and 2004.

The annual and seasonal WS_{max} in China during 2046–2065 and 2080–2099 are likely to decrease consistently relative to those of the 1981–2000 period, as projected by the GFDL_CM2_0, MRI_CGCM2, and EBGCM models. The three models also project that the annual and seasonal reductions in WS_{max} in the 21st century will be much larger than those of WS_{avg} . In the 21st century, the decreasing maximum wind speed over China may be related to decreases in the intensity of the East Asian winter monsoon and the decline of cold wave frequency. In addition, the decreasing maximum wind speed over the southeast coastal areas of China may be related to the decreas-

ing number of tropical cyclones over the Northwest Pacific Ocean.

REFERENCES

- Bloom, A., V. Kotroni, and K. Lagouvardos, 2008: Climate change impact of wind energy availability in the eastern Mediterranean using the regional climate model PRECIS. *Nat. Hazard Earth Sys.*, **8**, 1247–1257.
- Buech, C., C. Ulrich, and H. Stefan, 2003: Impacts of global warming on changes in the East Asian monsoon and the related river discharge in a global time-slice experiment. *Climate Res.*, **24**, 47–57.
- China Meteorological Administration (CMA), 2003: *Ground Surface Meteorological Observation*. China Meteorological Press, Beijing, 157 pp. (in Chinese)
- Cook, K. H., and E. K. Vizy, 2006: Coupled model simulations of the western African monsoon system: The 20th century simulations and the 21st century predictions. *J. Climate*, **19**, 3681–3703.
- Ding, R. Q., J. P. Li, S. G. Wang, et al., 2005: Decadal change of the spring dust storm in Northwest China and the associated atmospheric circulation. *Geophys. Res. Lett.*, **32**, L02808, doi: 10.1029/2004GL021651.
- Ding Yihui, Zhang Jin, and Song Yafang, 2002: Changes in weather and climate extreme events and their association with the global warming. *Meteor. Mon.*, **28**(3), 3–7. (in Chinese)
- Emanuel, K. A., 2005: Increasing destructiveness of tropical cyclones over the past 30 years. *Nature*, **436**, 686–688.
- Gao Xuejie, Zhao Zongci, and Filippo Giorgi, 2002: Changes of extreme events in regional climate simulations over East Asia. *Adv. Atmos. Sci.*, **19**(5), 927–942.
- , Lin Yiye, and Zhao Zongci, 2003: Impacts of greenhouse effect on typhoon over China as simulated by a regional climate model. *J. Trop. Oceanogr.*, **22**(4), 77–83. (in Chinese)
- Guo Qiyun, 1983: The summer monsoon intensity index in East Asia and its variation. *Acta Geogr. Sinica*, **38**(3), 207–217. (in Chinese)
- , Cai Jingning, Shao Xuemei, et al., 2004: Studies on the variations of East Asian summer monsoon during AD 1873–2000. *Chinese J. Atmos. Sci.*, **28**(2), 206–215. (in Chinese)
- Guo Yufu, Yu Yongqiang, Liu Xiyang, et al., 2001: Simulation of climate change induced by CO₂ increasing for East Asia with IAP/LASG GOALS model. *Adv. Atmos. Sci.*, **18**(1), 53–66.
- Hao, Y. B., H. S. Niu, Y. F. Wang, et al., 2011: Rainfall variability in ecosystem CO₂ flux studies. *Climate Res.*, **46**, 77–83, doi: 10.3354/cr00975.
- Hu Yamin and Song Lili, 2009: Climatologically statistical features of typhoon season parameters of tropical cyclones land falling in China. *Adv. Climate Change Res.*, **5**(2), 90–94. (in Chinese)
- Hu, Z., B. Lennart, and A. Klaus, 2000: Impact of the global warming on the Asian winter monsoon in a coupled GCM. *J. Geophys. Res.*, **105**, 4607–4624.
- IPCC, 2007: *Climate Change 2007: The Physical Science Basis*. Contribution of Working Group I to the Fourth Assessment Report of the Intergovernmental Panel on Climate Change. Solomon, S., D. Qin, M. Manning, et al., Eds. Cambridge University Press, Cambridge, United Kingdom and New York, NY, USA, 996 pp.
- James, B. E., P. K. James, and H. J. Thomas, 2008: The increasing intensity of the strongest tropical cyclones. *Nature*, **455**(4), 92–95.
- Jiang Ying, Luo Yong, Zhao Zongci, et al., 2009a: Evaluation of wind speeds in China as simulated by global climate models. *Acta Meteor. Sinica*, **67**(6), 1020–1029. (in Chinese)
- , —, —, et al., 2009b: Review of research on wind resources changes in China and in the world. *Sci. Tech. Rev.*, **27**(13), 96–104. (in Chinese)
- , —, —, et al., 2010a: Changes in wind speed over China during 1956–2004. *Theor. Appl. Climatol.*, **99**(3), 421–430. doi: 10.1007/s00704-009-0152-7.
- , —, —, et al., 2010b: Projections of wind changes for the 21st century in China by three regional climate models. *Chinese Geogr. Sci.*, **20**(3), 226–235. doi: 10.1007/s11769-010-0226-6.
- , —, —, et al., 2010c: Projection of wind speed changes in China in the 21st century by climate models. *Chinese J. Atmos. Sci.*, **34**(2), 323–336. (in Chinese)
- , —, —, et al., 2010d: Projection of wind power density in China in the 21st century by climate models. *Resour. Sci.*, **32**(4), 640–649. (in Chinese)
- Knutson, T. R., and R. E. Tuleya, 1999: Increased hurricane intensities with CO₂-induced warming as simulated using the GFDL hurricane prediction system. *Climate Dyn.*, **15**(7), 503–519.

- , E. T. Robert, W. X. Shen, et al., 2001: Impact of CO₂-induced warming on hurricane intensities as simulated in a hurricane model with ocean coupling. *J. Climate*, **14**, 2458–2468.
- Lei Xiaotu, Xu Ming, and Ren Fumin, 2009: A review on the impacts of global warming on tropical cyclone activities. *Acta Meteor. Sinica*, **67**(5), 679–688. (in Chinese)
- Li Yan, Wang Yuan, and Tang Jianping, 2007: Temporal and spatial variation characteristics in near-surface wind energy in China. *J. Nanjing Univ. (Natural Science)*, **43**(3), 61–72. (in Chinese)
- Li Zhen, Yan Zhongwei, Tu Kai, et al., 2011: Changes in wind speed and extremes in Beijing during 1960–2008 based on homogenized observations. *Adv. Atmos. Sci.*, **28**(2), 408–420.
- Phillips, T. J., and P. J. Gleckler, 2006: Evaluation of continent precipitation in the 20th century climate simulation: The utility of multi-model statistics. *Water Resource Res.*, **42**, W03202, doi: 10.1029/2005WR004313.
- PRC Committee of Editing Climate Change Assessment Report (PRCC), 2007: *China's National Assessment Report on Climate Change*. Scientific Press, Beijing, 422 pp. (in Chinese)
- Pryor, S. C., R. J. Barthelmie, and E. Kjellstrom, 2005: Potential climate change impact on wind energy resources in northern Europe: Analyses using a regional climate model. *Climate Dyn.*, **25**, 815–835.
- Qian, W. H., L. S. Quan, and S. Y. Shi, 2002: Variations of the dust storm in China and its climatic control. *J. Climate*, **15**, 1216–1229.
- , and X. Lin, 2004: Regional trends in recent temperature indices in China. *Climate Res.*, **27**(2), 119–134, doi: 10.3354/cr027119.
- and Zhang Weiwei, 2007: Changes in cold wave events and warm winter in China during the last 46 years. *Chinese J. Atmos. Sci.*, **31**(6), 1266–1278. (in Chinese)
- Ren, F. M., L. G. Wu, W. J. Dong, et al., 2006: Changes in tropical cyclone precipitation over China. *Geophys. Res. Lett.*, **33**, L20702, doi: 10.1029/2006GL027951.
- Ren Guoyu, Guo Jun, Xu Minzhi, et al., 2005: Climate changes of China's mainland over the past half century. *Acta Meteor. Sinica*, **63**(6), 942–956. (in Chinese)
- Rockel, B., and K. Woth, 2007: Future changes in near surface wind speed extremes over Europe from an ensemble of RCM simulations. *Climatic Change*, doi: 10.1007/s10584-006-9227-y.
- Shi Neng, 1996: Features of the East Asian winter monsoon intensity on multiple time scale in recent 40 years and their relation to climate. *J. Appl. Meteor. Sci.*, **7**(2), 175–182. (in Chinese)
- Wang Cunzhong, Niu Shengjie, and Wang Lanning, 2009: Multi-time scale variation of stand-dust storm in China during 1958–2007. *Trans. Atmos. Sci.*, **32**(4), 507–512.
- Wang Shaowu and Ye Jinlin, 1995: An analysis of global warming during the last one hundred years. *Chinese J. Atmos. Sci.*, **19**(5), 545–553. (in Chinese)
- , Gong Daoyi, and Zhou Tianjun, 2001: Twentieth-century climatic warming in China in the context of the Holocene. *Holocene*, **11**, 313–321.
- Wang Xiaoling and Zhai Panmao, 2004: The spatial and temporal variations of spring dust storms in China and its associations with surface winds and sea level pressures. *Acta Meteor. Sinica*, **62**(1), 96–103. (in Chinese)
- , Wang Yongmei, Ren Fumin, et al., 2006: Interdecadal variations in frequencies of typhoon affecting China during 1951–2004. *Adv. Climate Change Res.*, **3**(10), 66–69.
- Wang Xinmin, Zou Xukai, and Zhai Panmao, 2007: Researches on extratropical cyclone variability in the Northern Hemisphere. *Adv. Climate Change Res.*, **3**(3), 154–161. (in Chinese)
- Wang Xiuping and Zhang Yongning, 2006: Interdecadal change of the landing tropical cyclone tracks over China. *J. Dalian Maritime Univ.*, **32**(3), 41–45. (in Chinese)
- Wang Zhunya, Ding Yihui, He Jinhai, et al., 2004: An updating analysis of the climate changes in China in recent 50 years. *Acta Meteor. Sinica*, **62**(2), 228–236. (in Chinese)
- and —, 2006: Climate change of the cold wave frequency of China in the last 53 years and the possible reasons. *Chinese J. Atmos. Sci.*, **30**(6), 1068–1076. (in Chinese)
- Wei Fengying, 1999: *The Technologies of Statistics Diagnosis and Forecast in Modern Climate*. China Meteorological Press, Beijing, 269 pp. (in Chinese)
- Wei Junhong and Lin Zhaohui, 2009: The leading mode of wintertime cold wave frequency in northern China during the last 42 years and its association with Arctic oscillation. *Atmos. Oceanic Sci. Lett.*, **2**(3), 130–134.

- World Meteorological Organization (WMO), 2004: Guidelines on Quality Control Procedures for Data from Automatic Weather Stations. CBS/OPAG2IOS/ ET AWS23/DOC, **4**(1), 1–9.
- Wu, L. G., B. Wang, and Scott A. Braun, 2007: Implications of tropical cyclone power dissipation index. *Int. J. Climatol.*, doi: 10.1002/joc.1573.
- Xu, M., C. P. Chang, C. B. Fu, et al., 2006: Steady decline of East Asian monsoon winds in 1969–2000: Evidence from direct ground measurements of wind speed. *J. Geophys. Res.*, **111**, D24111, doi: 10.1029/2006JD007337.
- Yan Zhongwei and Yang Chi, 2000: Geographical patterns of extreme climate changes in China during recent decades. *Climatic Environ Res.*, **5**(3), 267–372. (in Chinese)
- Yang, H. L., Y. L. Xu, L. Zhang, et al., 2010: Projected change in heat waves over China using the PRECIS climate model. *Climate Res.*, **42**(1), 79–88, doi: 10.3354/cr00860.
- Zhang Aiyong, Ren Guoyu, Guo Jun, et al., 2009: Change trend analyses on upper-air wind speed over China in past 30 years. *Plateau Meteor.*, **28**(3), 680–687. (in Chinese)
- Zhang Li, Ding Yihui, and Sun Ying, 2008: Test of the East Asian summer monsoon rainfall simulated by global sea-air coupling model. *Chinese J. Atmos. Sci.*, **32**(2), 261–270. (in Chinese)
- Zhao Ping and Zhou Zijiang, 2005: East Asian subtropical summer monsoon index and its relationships to rainfall. *Acta Meteor. Sinica*, **63**(6), 933–941. (in Chinese)
- Zhao Zongci, Luo Yong, Gao Xuejie, et al., 2007: Projections of typhoon changes over the western North Pacific Ocean for the 21st century. *Adv. Climate Change Res.*, **3**(3), 158–161.
- Zhou, T. J., and R. C. Yu, 2006: Twentieth century surface air temperature over China and the globe simulated by coupled climate models. *J. Climate*, **19**(22), 5843–5858.
- Zhou Tianjun, Li Lijuan, Li Hongmei, et al., 2008: Progress in climate change attribution and projection studies. *Chinese J. Atmos. Sci.*, **32**(4), 906–922. (in Chinese)
- Zhu, J. H., and X. Z. Liang, 2005: Regional climate model simulation of U.S. soil temperature and moisture during 1982–2002. *J. Geophys. Res.*, **110**, D24110, doi: 10.1029/2005JD006472.